Properties of Aging FeCl2 Clusters Grown in Supercritical Water Investigated by Molecular Dynamics Simulations

ARTICLE *in* THE JOURNAL OF CHEMICAL PHYSICS · JANUARY 2010

Impact Factor: 2.95 · DOI: 10.1063/1.3270158 · Source: PubMed

2 AUTHORS, INCLUDING:

Bjørn Kvamme
University of Bergen
364 PUBLICATIONS **1,647** CITATIONS

Properties of aging $FeCl_2$ clusters grown in supercritical water investigated by molecular dynamics simulations

Norbert Lümmen[a] and Bjørn Kvamme
Department of Physics and Technology, University of Bergen, Allégaten 55, 5007 Bergen, Norway

(Received 15 September 2009; accepted 10 November 2009; published online 5 January 2010)

We have investigated the growth and properties of $FeCl_2$ nanoparticles from supercritical water by molecular dynamics simulations. After particle growth had finished after less than 250 ps, selected properties of the aging clusters such as structure, shape, and amount of crystal water content were analyzed for up to 1.5 ns simulation time. Very quick growth and shape relaxation of the clusters are observed. The developments of cluster size, radius of gyration, and moments of inertia with time have been analyzed. The number of water molecules that are part of the clusters is found to increase almost linearly with cluster size. The shape relaxation of the clusters happens faster after cluster-cluster collisions and faster than the time needed for the clusters to reorganize their structure and attain a highly ordered ground state structure. The development of the cluster structure with time as analyzed by radial distribution functions shows hardly any changes over time, but shows significant variations with system temperature and system density. © *2010 American Institute of Physics*. [doi:10.1063/1.3270158]

I. INTRODUCTION

Supercritical water (SCW) is a solvent appearing in both nature[1,2] and industrial processes.[3–6] Above its critical point (T_c=647 K, p_c=22 MPa, and ρ_c=0.322 g/cm^3),[7] the solvation properties of water change due to a smaller degree of hydrogen bonded structure. Experiments have shown that ions solvated in water tend to aggregate under such conditions.[8] SCW is, like many other supercritical fluids, a suitable solvent in materials processing, pharmacy, and food industry[3–6] because its solvation properties can be controlled by the applied temperature and pressure above the critical point.

Supercritical water oxidation (SCWO) is a technology to purify water contaminated with organic waste under addition of molecular oxygen.[9] Waste water containing halogenated organic molecules is difficult to treat with this process because the ions will associate and form salt particles. The precipitation of solid salt particles leads to plugging of pipelines and reactors. This effect has also the potential to be exploited in seawater desalination processes if the ionic association can be controlled. Treatment of halogenated wastewater still poses problems within SCWO technology even though newer reactor designs are able to cope better with salt precipitation.[10,11] Molecular simulations can assist in the development of a fundamental understanding of the particle formation process and the involved dynamics.

Natural hydrothermal fluids are rich in ionic species[12–14] such as, for example, Fe^{2+} and Mn^{2+}. Seawater changes its composition with changing temperature and pressure due to exchange processes with the surrounding rock[15] while it circulates through porous seafloor. The pressures are high enough for seawater to attain the supercritical state if a heat source like intrusive basalt is present below water depths of more than 2800 m. The formation of (sub-) seafloor ore deposits such as metal-rich brines or metalliferous sediments[16] is then the result of natural salt particle formation. Experiments and computer simulations by Hovland *et al.*[1,2] recently verified the aggregation of NaCl due to subsurface boiling of critical seawater. Formation of large aggregates and deposits of metal salts, if the hydrothermal fluid feed is rich in metal ions, is therefore very likely.

Simulation studies of salts of divalent metal ions in water have been carried out by several groups on, for example, aqueous $ZnCl_2$ solutions at high pressure and temperature.[17] $SrCl_2$ was studied by molecular dynamics (MD) simulations at both ambient[18] and hydrothermal temperatures.[19] A common observation in these investigations is the fast aggregation of ions of unlike charge in water in the supercritical state.

In this work we study aging of $FeCl_2$ nanoparticles grown in SCW[20,21] for up to 1.5 ns. MD simulations with 120 Fe^{2+} ions and 240 Cl^- ions distributed in cubic simulation volumes containing 2048 water molecules were carried out at different state conditions in the supercritical region of the phase diagram of water. The amount of ions yields an $FeCl_2$ content of 29.2 wt % and corresponds to an ion to water molecule ratio of 0.176 (=360 ions/2048 water molecules). We were interested in the further development of structural properties of the grown $FeCl_2$ clusters after we had investigated these systems before in terms of nucleation[20] and growth.[21] Nucleation and growth of $FeCl_2$ clusters were terminated at times of 250 ps or less.[21] The extended simulation time of 1.5 ns was chosen to investigate the development of structural properties with time.

[a]Electronic mail: norbert@ift.uib.no and norbert.luemmen@uib.no.

TABLE I. Stillinger criteria for the detection of clusters.

Atom/ion pairs	Distance/nm
Fe^{2+}–Fe^{2+}, Fe^{2+}–Cl^-, Cl^-–Cl^-	0.3225
O–Fe^{2+}	0.32
O–Cl^-	0.43
O–O	0.38

II. METHODS

The MD simulations program package M.DYNAMIX 4.3 (Ref. 22) was used along with the trajectory analysis tool *tranal* included in this package. The latter was modified to allow for the detection of clusters by means of the Stillinger criterion.[23] This simple geometric cluster criterion marks two atoms belonging to the same cluster if they lie within a certain given distance from each other. These distance criteria are taken as the first minima in corresponding radial distribution functions (RDFs).[21] The actual distances used are listed in Table I. The presence of water molecules is important both as solvent during growth[24] and as solvent and crystal water in the clusters. It thus has an impact on the shape and structure of the growing particles.[25] The role of crystal water, like it is found in bulk iron(II) chloride tetrahydrate ($FeCl_2 \cdot 4H_2O$) grown from aqueous solutions,[26] was accounted for by allowing an ion to be part of a cluster if a single water molecule connected them by means of the applied distance criteria. However, the cluster size was just counted by the number of ions constituting a cluster.

The interaction between the atoms constituting the 2048 rigid water molecules was modeled by the extended simple point charge (SPC/E) model.[27] The SHAKE algorithm[28] was used to keep the internal bond lengths of the water molecules fixed. The SPC/E model was found to give good results in several studies on salt containing solutions at high temperatures and pressures.[17,29] It is also able to closely reproduce the critical density and critical temperature of water.[30–32] A combination of the short-ranged Lennard-Jones potential and long-ranged Coulomb potential was chosen for the interaction between the ions (120 Fe^{2+} ions, 240 Cl^- ions) and the ions and water molecules. Cross interactions involving the Lennard-Jones parameters are calculated by the Lorentz–Berthelot rules.[33] We used the parameters of Smith and Dang[29] for the Cl^- ions and our own parameters for the Fe^{2+} ions.[21]

In the simulations a time step of 1 fs was used to integrate the Newton's equations of motion of all atoms and ions by a simple leap frog algorithm.[33] Within M.DYNAMIX 4.3 (Ref. 22) the intermolecular forces of the Lennard-Jones type are cut beyond a cutoff radius, which we set to 1.0 nm, and set to zero beyond the cutoff. The Ewald-summation method[33] (real part cutoff at 1.0 nm, damping constant $=\pi/10$) was applied to treat the long range forces originating from the partial charges on the water molecules and the ionic charges. Furthermore, standard methods in MD simulations such as neighbor lists, periodic boundary conditions, and minimum image convention were applied[33] to reduce the demand on computational resources.

The temperature in the simulated systems was controlled by a heat bath thermostat (based on a Nosé–Hoover thermostat[34,35]), which acted exclusively on the water molecules. This method of temperature control is closer to the experimental situation where particles are usually grown in a solvent or a carrier gas atmosphere, which also acts as a heat bath. We applied this concept successfully in our studies on NaCl and $FeCl_2$ salt cluster formation in SCW.[20,36,37]

We have calculated radii of gyration of clusters and their principal moments of inertia. The radius of gyration of a cluster is given by

$$r_{\mathrm{gyr}} = \sqrt{\frac{\sum_{i=1}^{N} (\vec{r}_i - \vec{r}_{\mathrm{c.o.m.}})^2}{N}}, \tag{1}$$

where $\vec{r}_{\mathrm{c.o.m.}}$ is the location of the cluster's center of mass and $\vec{r}_i$ is the location of the ith atom in a cluster of N atoms.

III. RESULTS AND DISCUSSION

Figure 1(a) shows the development of the size of the largest cluster versus time for a range of systems at different state conditions. The largest cluster, which can change its identity over the course of a simulation, is chosen as a representative particle for all the other clusters in the systems. It undergoes the same processes like all the other clusters from nucleation toward a stable particle. The first 200 ps in the diagram are dominated by growth processes. Within this time frame, clusters form from single ions located in the solvent to clusters of ions. This proceeds at first by surface growth and addition of small molecules and later by cluster-cluster collisions. The latter causes the large steps in the curves on the vertical axis. Almost all ions present in the systems have aggregated into a single large cluster after 200 ps simulation time. The aggregation is driven by the small solubility of ions in SCW at the given state conditions. They are located well above the critical point of pure water[7] and as a consequence, the dielectric constant of water is very low, which promotes the association of ions into charge neutral molecules or larger aggregates. There are only very small size fluctuations visible after cluster growth is completed. These are caused by reorganizing processes in the cluster surface, during which single ions can become temporarily detached from the cluster. This can be due, for example, to repulsive forces exerted during the relocation of a countercharged ion in the near vicinity of a loosely bound ion. The detached ion gets reattached to the cluster as it is unlikely to be soluble in the surrounding solvent at the given conditions.

The dynamics of temporary ion detachment is also reflected in the small fluctuations in cluster composition shown in Fig. 1(b) in the same time range. The fluctuations shortly after the beginning of the simulation represent the large fluctuations in cluster composition during the time of growth. The growing clusters pass through a sequence of nonequilibrium structures as both single ions and molecules of different sizes and compositions get attached to the cluster during growth. After cluster growth is complete and all available ions in the system have aggregated into one cluster, the largest cluster attains the Fe^{2+} mole fraction of the system, which is $\frac{1}{3}$ (water molecules are neglected). Figure 1(c) shows that the Fe^{2+} mole fraction of the largest cluster is already close

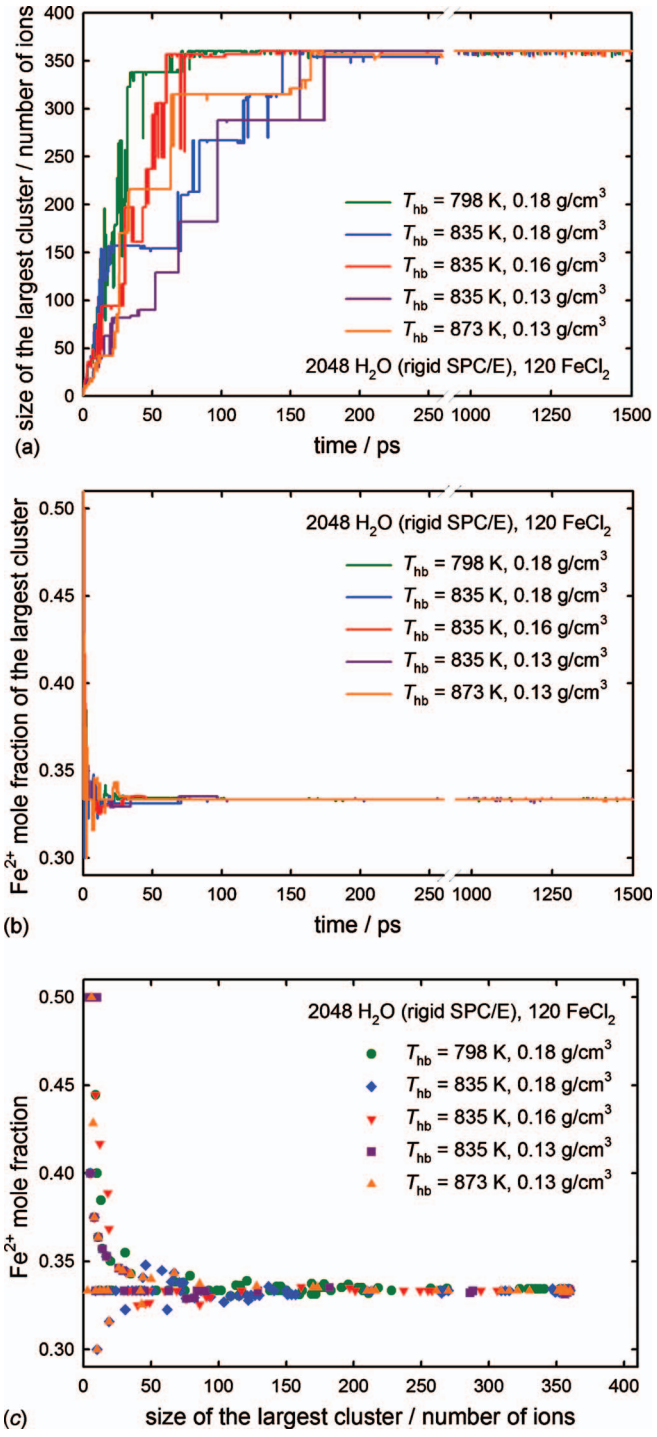

FIG. 1. (a) Development of the size of the largest cluster with time given by the number of ions. (b) Fe^{2+} mole fraction of the largest cluster vs time. (c) Fe^{2+} mole fraction of the largest cluster vs its size in number of ions.

to the system value at a cluster size of about 80 ions. Further collisions lead only to small fluctuations in the cluster composition. This is a hint that also the majority of the other clusters in the system have an Fe^{2+} mole fraction close to $\frac{1}{3}$.

Figure 2(a) shows the number of water molecules that are part of the largest cluster in the system. Their number grows approximately linearly with the number of ions in the cluster [Fig. 2(b)]. It increases during particle collisions and decreases with time at constant particle size until a new equilibrium amount of water molecules in and around a cluster is reached. The number of water molecules is largest for low heat bath temperature and high system density (about 400 water molecules), and smallest for high heat bath temperature and low system density, for which a number of about 290 water molecules were observed. The faster growth observed at the higher system density obviously results in a larger amount of water molecules included in the cluster interior and around the largest cluster in the system. Fluctuations in the number of water molecules of up to 50 can be observed. Even though the growth of the cluster is complete after 200 ps the number of water molecules varies dynamically.

The RDFs (Figs. 3 and 4), calculated from configuration data every 250 ps, show hardly any development with time. The first peak in the O-ion curve (Fig. 3) is the $O-Fe^{2+}$ peak, which is located at 0.207 nm for all the systems we investigated. The second peak in the O-ion RDF is the $O-Cl^-$ peak. It is located at 0.327 nm in all studied systems. The ion-ion RDF (Fig. 4) has its first peak (which is the first $Fe^{2+}-Cl^-$ peak) at 0.243 nm in all systems. The first minimum lies at 0.325 nm and the second peak (which is also the first Cl^--Cl^- peak) at 0.383 nm. The third peak in the combined ion-ion RDF lies at the first peak of the $Fe^{2+}-Fe^{2+}$ RDF at 0.475 nm. We have previously reported on these RDFs in more detail.[21] We found good agreement of the location of the first peaks and minima between our simulation results[21] and experimental observations[38,39] for both oxygen-ion RDFs and the ion-ion RDFs. These experimental investigations employed different methods of x-ray absorption spectroscopy on various Fe^{2+} and Fe^{3+} chloride solutions[38] and neutron diffraction studies of iron(II) chloride tetrahydrate ($FeCl_2 \cdot 4H_2O$).[39] The observed $O-Fe^{2+}$ distance of 0.207 nm fits very well to x-ray absorption studies by Apted[38] and the recent study by Testemale *et al.*,[40] which employs the same type of methods. The water molecules have an influence on the location of the different peaks if one compares, for example, the $Fe^{2+}-Cl^-$ distance to experimental results obtained in studies of $FeCl_2$ molecule structure in host crystals at cryogenic temperatures. X-ray absorption fine structure spectroscopy yields a distance of 0.2156 nm in a CH_4 host and 0.2207 nm in a N_2 host.[41] A value of 0.2151 nm was obtained by combined gas phase electron diffraction and vibrational spectroscopic analysis.[42] This is considerably shorter than the value of 0.243 nm, which we obtain for the clusters. The likewise shorter $Fe^{2+}-Cl^-$ distance of 0.231 nm observed in the study by Testemale *et al.*[40] is probably a consequence of the different compositions of the studied solutions, which also included lithium ions and a very high chloride concentration.

The changes with time between the RDFs shown in Figs. 3(a) and 3(b) are small. While the peak locations do not change with time, the relative height of the curves is slightly different after 1.5 ns compared to 0.25 ns. The heights of the first peaks are found between 12.5 and 15 at 1.5 ns while the one for T_{hb}=835 K and 0.13 g/cm^3 reached nearly 16 after 0.25 ns. The curves' relative position on the vertical axis and beyond the second peak is conserved while the distances between them are getting more equal.

The succession of peak heights increase with increasing

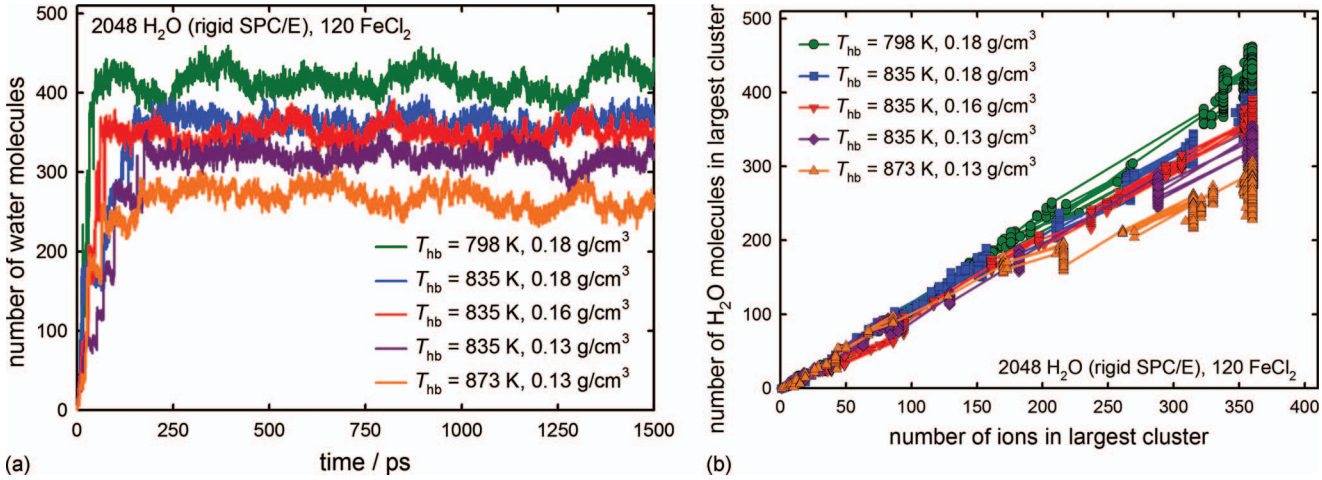

FIG. 2. (a) Development of the number of water molecules being part of the largest cluster in the system with time. A water molecule is marked as being part of an ionic cluster if it is a neighbor to at least two ions in that cluster. (b) Development of the number of water molecules in the largest cluster vs its size. The dependency appears almost linear.

heat bath temperature and decreasing system density in case of the ion-ion [Fig. 4(a)] and Fe^{2+}–Cl^- RDFs [Fig. 4(b)]. This picture does not change with time compared to the situation after 0.25 ns.[21] It is interesting to note, that the height of the first and second peaks in the ion-ion RDF shown in Fig. 4(c) slightly decreases with time. No specific trend with progressing time can be found for the other peaks. However, the curves tend to be not as smooth as for the distance interval up to about 0.45 nm. This could be related to the dynamics of the water molecules observed in Fig. 2(a) and that this leads to continuous rearrangements of the cluster structure on very short distances. There is also no visible trend for the curve height with increasing simulation time.

The coordination numbers of the different constituents hardly change as their values are directly related to the RDFs. The Fe^{2+}–Cl^- coordination numbers range between 1.2 and 1.5. The curves lie at slightly larger values within this interval with increasing heat bath temperature. There is, however, no clear trend with increasing simulation time. This probably reflects the observed changes in number of water molecules over time and their influence on the coordination of the ions. The coordination numbers for the Fe^{2+}–O pair lie between 2.3 and 2.8 and decrease with increasing heat bath temperature. In an ideal $FeCl_2$ crystal, even if it contains water, one would expect a coordination number of 2 for the Fe^{2+}–Cl^- combination. It is very likely, that the large number of water molecules, which are a part of the cluster, lower this value. The hydrated ions in the cluster surface have strong influence on the overall coordination numbers as the clusters are of a size, where most of the ions are located on the cluster surface. Disorder in the cluster itself also has a strong influence on the coordination number. The decreasing Fe^{2+}–O coordination number with increasing heat bath temperature could reflect the tendency toward a smaller amount of water molecules in the cluster. This is already visible from the curve in Fig. 2(a). As the number of water molecules does neither continuously increase or decrease with time has the consequence, that there is no specific development with time for this property.

The very small changes in the cluster structure over a course of more than a nanosecond since the conclusion of cluster growth as analyzed from RDFs and coordination numbers are a direct consequence of its fast speed. The size of the critical cluster in the investigated systems has been

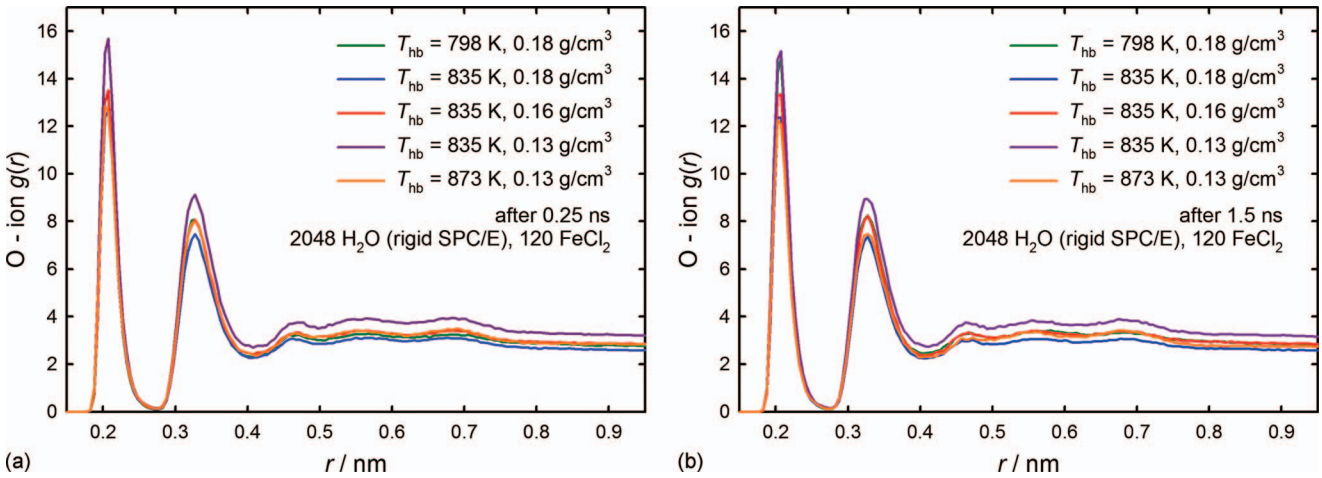

FIG. 3. (a) Radial oxygen-ion distribution functions for all systems after 0.25 ns. (b) Radial oxygen-ion distribution functions for all systems after 1.5 ns.

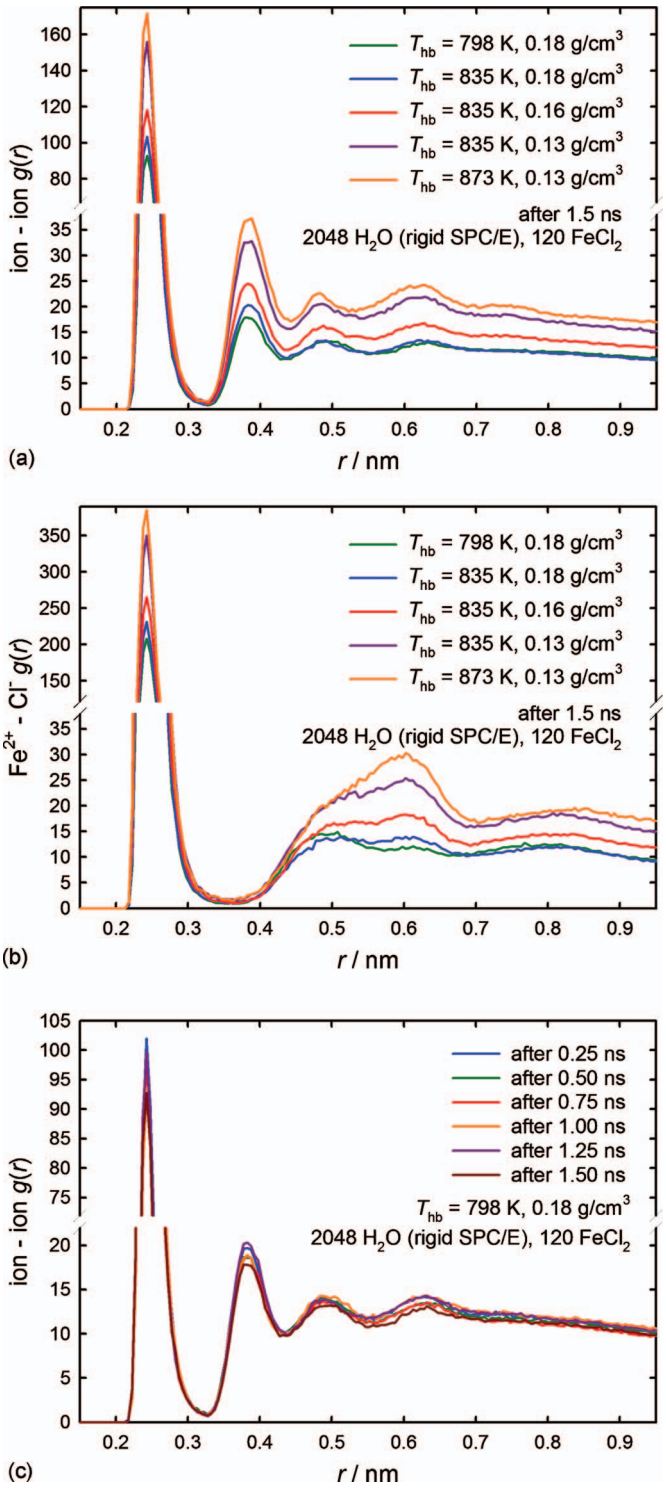

FIG. 4. (a) Radial ion-ion distribution functions for all systems after 1.5 ns. (b) Radial Fe^{2+}–Cl^- distribution functions for all systems after 1.5 ns. (c) Development of the radial ion-ion distribution function with time for the system at T_{hb}=798 K and ρ=0.18 g/cm^3.

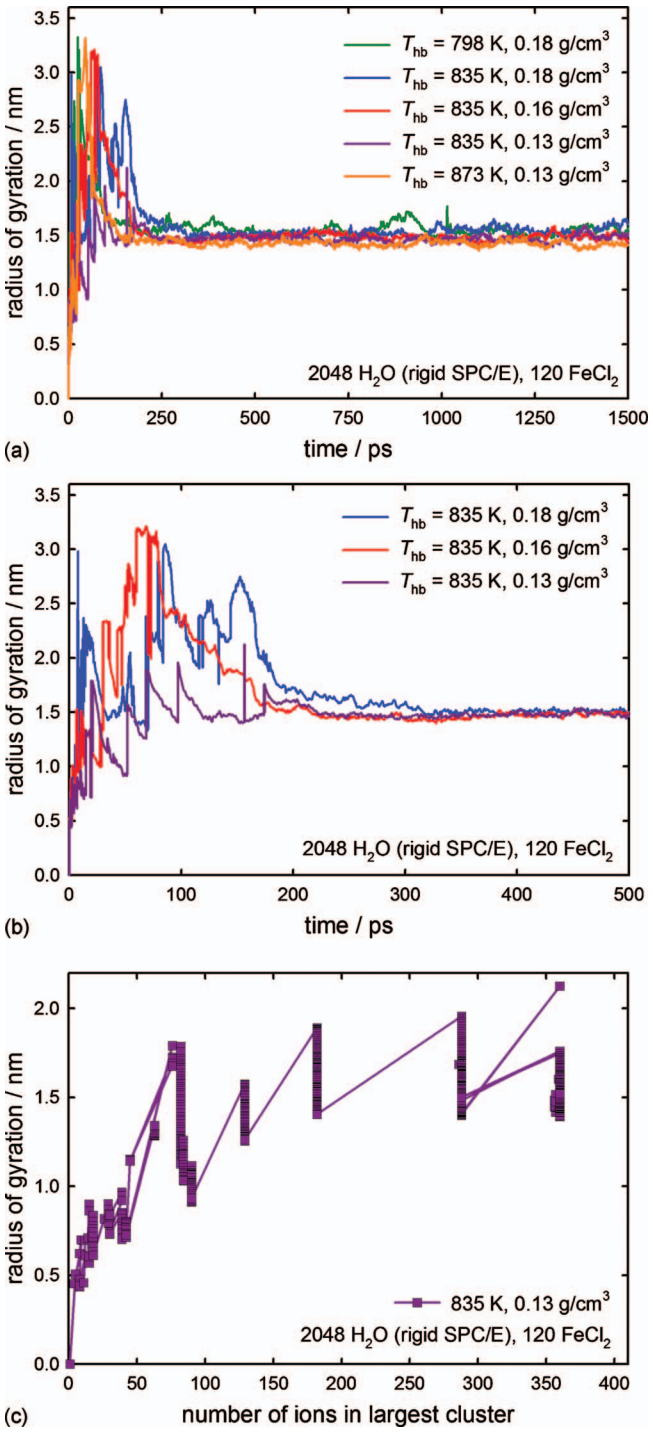

FIG. 5. (a) Development of the radius of gyration with time for the largest cluster in all investigated systems. (b) Close-up on the size development for the largest cluster in the three systems at 835 K heat bath temperature. (c) Development of the radius of gyration of the largest cluster with its size in one of the systems. The relaxations to a smaller value after coalescence with another cluster are clearly visible.

estimated to be 12–15 ions.[20] Cluster growth not only proceeds via attachment of single ions but also by collisions with other instable clusters of subcritical size. Fe^{2+}–Cl^- molecules, charge-neutral $(FeCl_2)_n$ molecules are highly abundant during the initial phase of nucleation and cluster growth. As the attachment of these building blocks completes within a very short time scale, the clusters proceed along a path of nonequilibrium structures during growth. The next collision with either ion or cluster happens already before the cluster had the time to relax into a ground-state structure at the given cluster composition and state conditions. The different sizes of the ions and the inclusion of water molecules also have an impact on the structural relaxation processes. The cluster structure therefore can get tem-

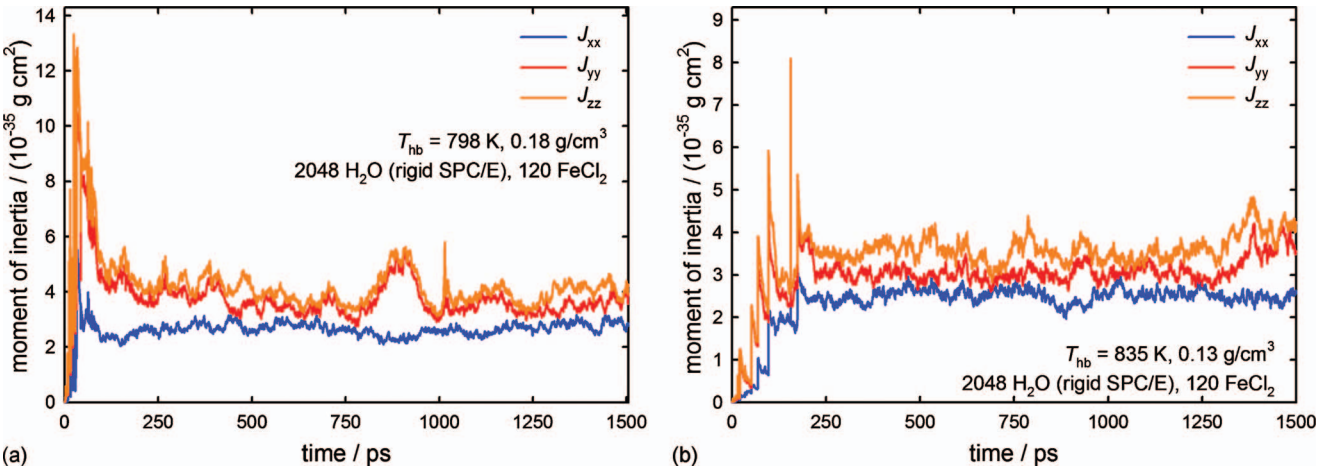

FIG. 6. (a) Development of the principal moments of inertia of the largest cluster in the system with time at T_{hb}=798 K and ρ=0.18 g/cm^3; (b) Same as in (a) but for the largest cluster in the system at T_{hb}=835 K and ρ=0.13 g/cm^3.

porarily locked into a metastable structure and morphology with high energy barriers to structural reorganization toward structures of lower energy.

The radius of gyration [Eq. (1)], which is a measure for the particle size, is estimated to 1.5 nm from the graphs in Figs. 5(a) and 5(b). The corresponding curves for times after the completion of cluster growth usually only exhibit small fluctuations. Jumps of up to a nanometer and quick relaxation toward smaller values can be observed in the close-up onto the first 500 ps for the systems at T_{hb}=835 K in Fig. 5(b). Values of up to 3.3 nm are reached during cluster-cluster collisions [T_{hb}=798 K, Fig. 5(a)], but the clusters are not spherical-like at this stage. However, although the cluster shapes seem to relax very quickly after cluster-cluster collisions, the same cannot be said for the cluster structure itself, as discussed above. Similar values and behavior of the radius of gyration were found in a study of $SrCl_2$ clusters grown in MD simulations at hydrothermal conditions.[19] The difference in the number of ions applied in the two different studies (46 $SrCl_2$ versus 120 $FeCl_2$) is reflected in the slightly larger radii for the $FeCl_2$ clusters. The diagram in Fig. 5(c), where the r_{gyr} is plotted versus the number of ions in the largest cluster clearly shows the size relaxations after collisions by the vertical bars of data points, while the jumps in cluster size are visible from the gaps between the bars of data points on the horizontal axis.

The development of the cluster shape with time can be traced by the principal moments of inertia for a given cluster (Fig. 6). In most cases, two of the moments show nearly the same values and development over time while the third one shows a different behavior and a smaller value compared to the other two [Fig. 6(a)]. This could be a hint to a deviation from an ideal spherical-like cluster shape as a result of an incomplete coalescence process after collision with another cluster. An exception from this behavior was also observed, where all three values of the principal moments of inertia are different [Fig. 6(b)]. In general, the three different moments of inertia converge toward a common value where the time scale is the same for the two moments with similar value and faster than for the third and smaller moment. Comparison with the aforementioned $SrCl_2$ clusters[19] yields similar behavior for clusters of the two different substances. The larger values of the moments of inertia for the $FeCl_2$ clusters are due to the slightly larger clusters and the larger amount of Fe^{2+} ions (120 compared to 46 Sr^{2+}) even though their weight is only roughly 64% of that of the Sr^{2+} ions. The relaxation of the principal moments in x- and y-direction, J_{xx} and J_{yy}, in Fig. 6(a) is faster than the relaxation observed after cluster collisions for the $SrCl_2$ particles in cases where almost all ions have aggregated into a single large cluster.

The observed fast relaxations of both radius of gyration and moments of inertia are in contrast to the very slow relaxation processes of the cluster structure. The clusters are trapped in metastable structural states as a consequence. Numerical simulations of fast growth of charged colloids support this interpretation.[43] The transition into the final structure can therefore lie beyond the time scale that can be covered with the conducted MD simulations. It may also be necessary to induce such a transition by changing the state conditions toward higher temperatures such that there is more energy available to overcome energy barriers.

IV. CONCLUSIONS

We have investigated the growth and properties of $FeCl_2$ nanoparticles from SCW by MD simulations for up to 1.5 ns simulation time. The number of water molecules that are part of the clusters increases almost linearly with cluster size during growth. The shape relaxation of the clusters happens faster after cluster-cluster collisions than the clusters have time to reorganize their structure and attain an ordered ground state structure. The development of the cluster structure with time as analyzed by RDFs shows hardly any changes over time, but differences with system temperature and system density. It is therefore highly likely, that the clusters get kinetically trapped in metastable structural states due to the fast growth from small molecular fragments of subcritical size and very fast shape relaxations after cluster-cluster collisions.

ACKNOWLEDGMENTS

This work was funded by the Deutsche Forschungsgemeinschaft (DFG) (Grant No. LU-1406/1-1). All simulations were carried out on the Linux cluster 'fimm' at the Bergen Center for Computational Science (BCCS, http://www.bccs.uib.no).

[1] M. Hovland, H. G. Rueslåtten, H. K. Johnsen, B. Kvamme, and T. Kuznetsova, Mar. Pet. Geol. **23**, 855 (2006).
[2] M. Hovland, T. Kuznetsova, H. Rueslåtten, B. Kvamme, H. K. Johnsen, G. E. Fladmark, and A. Hebach, Basin Res. **18**, 221 (2006).
[3] C. Aymonier, A. Loppinet-Serani, H. Reverón, Y. Garrabos, and F. Cansell, J. Supercrit. Fluids **38**, 242 (2006).
[4] F. Cansell, C. Aymonier, and A. Loppinet-Serani, Curr. Opin. Solid State Mater. Sci. **7**, 331 (2003).
[5] A. Kruse and E. Dinjus, J. Supercrit. Fluids **39**, 362 (2007).
[6] A. Kruse and E. Dinjus, J. Supercrit. Fluids **41**, 361 (2007).
[7] M.-C. Bellissent-Funel, J. Mol. Liq. **90**, 313 (2001).
[8] J. W. Tester, H. R. Holgate, F. J. Armellini, P. A. Webley, W. R. Killilea, G. T. Hong, and H. E. Berner, *Emerging Technologies in Hazardous Waste Management III*, American Chemical Society Symposium Series, edited by D. W. Tedder and F. G. Pohland (American Chemical Society, Washington, D.C., 1993), Vol. 518, pp. 35–76.
[9] M. Hodes, P. A. Marrone, G. T. Hong, K. A. Smith, and J. W. Tester, J. Supercrit. Fluids **29**, 265 (2004).
[10] P. A. Marrone, M. Hodes, K. A. Smith, and J. W. Tester, J. Supercrit. Fluids **29**, 289 (2004).
[11] K. Príkopský, B. Wellig, and Ph. R. von Rohr, J. Supercrit. Fluids **40**, 246 (2007).
[12] R. P. Lowell, P. A. Rona, and R. P. Von Herzen, J. Geophys. Res. **100**, 327, doi:10.1029/94JB02222 (1995).
[13] K. L. Von Damm, J. M. Edmond, B. Grant, C. I. Measures, B. Walden, and R. F. Weiss, Geochim. Cosmochim. Acta **49**, 2197 (1985).
[14] K. L. Von Damm, J. M. Edmond, C. I. Measures, and B. Grant, Geochim. Cosmochim. Acta **49**, 2221 (1985).
[15] D. A. Butterfield, I. R. Jonasson, G. J. Massoth, R. A. Feely, K. K. Roe, R. E. Embley, J. F. Holden, R. E. McDuff, M. D. Lilley, and J. R. Delaney, Philos. Trans. R. Soc. London, Ser. A **355**, 369 (1997).
[16] P. A. Rona, Science **299**, 673 (2003).
[17] D. J. Harris, J. P. Brodholt, J. H. Harding, and D. M. Sherman, Mol. Phys. **99**, 825 (2001).
[18] D. E. Smith and L. X. Dang, Chem. Phys. Lett. **230**, 209 (1994).
[19] I. M. Svishchev, A. Y. Zasetsky, and I. G. Nahtigal, J. Phys. Chem. C **112**, 20181 (2008).
[20] N. Lümmen and B. Kvamme, J. Supercrit. Fluids **47**, 270 (2008).
[21] N. Lümmen and B. Kvamme, J. Phys. Chem. B **112**, 15262 (2008).
[22] A. P. Lyubartsev and A. Laaksonen, Comput. Phys. Commun. **128**, 565 (2000).
[23] F. H. Stillinger, J. Chem. Phys. **38**, 1486 (1963).
[24] G. Mpourmpakis and D. G. Vlachos, Langmuir **24**, 7465 (2008).
[25] V. Gorshkov, A. Zavalov, and V. Privman, Langmuir **25**, 7940 (2009).
[26] D. D. Thornton, Phys. Rev. B **1**, 3193 (1970); J. N. McElearney, H. Forstat, and P. T. Bailey, Phys. Rev. **181**, 887 (1969).
[27] H. J. C. Berendsen, J. R. Gridera, and T. P. Stratsmaa, J. Phys. Chem. **91**, 6269 (1987).
[28] F. Graf, K. Loth, M. Rudin, M. Forster, T.-K. Ha, and Hs. H. Günthard, J. Phys. Chem. **23**, 327 (1977).
[29] D. E. Smith and L. X. Dang, J. Chem. Phys. **100**, 3757 (1994).
[30] J. P. Brodholt, Chem. Geol. **151**, 11 (1998).
[31] T. M. Hayward and I. M. Svishchev, Fluid Phase Equilib. **182**, 65 (2001).
[32] C. Nieto-Draghi, J. Bonet Avalos, and B. Rousseau, J. Chem. Phys. **118**, 7954 (2003).
[33] M. P. Allen and D. J. Tildesley, *Computer Simulation of Liquids* (Oxford University Press, Oxford, 1989).
[34] S. Nosé, Mol. Phys. **52**, 255 (1984).
[35] G. J. Martyna, D. J. Tobias, and M. L. Klein, J. Chem. Phys. **101**, 4177 (1994).
[36] N. Lümmen and B. Kvamme, Phys. Chem. Chem. Phys. **9**, 3251 (2007).
[37] N. Lümmen and B. Kvamme, Phys. Chem. Chem. Phys. **10**, 6405 (2008).
[38] M. J. Apted, G. A. Waychunas, and G. E. Brown, Geochim. Cosmochim. Acta **49**, 2081 (1985).
[39] J. J. Verbist, W. C. Hamilton, T. F. Koetzle, and M. S. Lehmann, J. Chem. Phys. **56**, 3257 (1972).
[40] D. Testemale, J. Brugger, W. Lie, B. Etschmann, and J.-L. Hazemann, Chem. Geol. **264**, 295 (2009).
[41] I. R. Beattie, M. D. Spicer, and N. A. Young, J. Chem. Phys. **100**, 8700 (1994).
[42] M. Hargittai, N. Yu. Subbotina, M. Kolonits, and Al. G. Greshikov, J. Chem. Phys. **94**, 7278 (1991).
[43] E. Sanz, C. Valeriani, D. Frenkel, and M. Dijkstra, Phys. Rev. Lett. **99**, 055501 (2007).